REPORT DOCUMENTATION PAGE

1. REPORT DATE (DD-MM-YYYY) 07/20/2007	2. REPORT TYPE FINAL	3. DATES COVERED (From - To) 06/06/2006 - 06/05/2007

4. TITLE AND SUBTITLE

Magnetostatically-Coupled Anisotropic Composite Magnets with Enhanced Remanence

5a. CONTRACT NUMBER

5b. GRANT NUMBER
N00173-06-1-G018

5c. PROGRAM ELEMENT NUMBER

6. AUTHOR(S)

Hadjipanayis, George, C.

5d. PROJECT NUMBER
63-0041-06

5e. TASK NUMBER

5f. WORK UNIT NUMBER

7. PERFORMING ORGANIZATION NAME(S) AND ADDRESS(ES)

Geraldine E. Hobbs
University of Delaware
Office of the Vice Provost for Research
210 Hullihen Hall
Newark DE 19716

8. PERFORMING ORGANIZATION REPORT NUMBER

PHYS 33212306000

Proposal #06000921

9. SPONSORING / MONITORING AGENCY NAME(S) AND ADDRESS(ES)

Dr. Shu-Fan Cheng
Naval Research Lab
4555 Overlook Ave. S.W.
Washington DC 20375   202-767-7271

10. SPONSOR/MONITOR'S ACRONYM(S)

11. SPONSOR/MONITOR'S REPORT NUMBER(S)

12. DISTRIBUTION / AVAILABILITY STATEMENT

"Approved for Public Release, Distribution is Unlimited"

13. SUPPLEMENTARY NOTES

14. ABSTRACT

The computer simulation confirmed a magnetostatic coupling between R-Fe-B matrix and thick Fe layers in hot-deformed composite magnets. However, enhancement in the remanence and maximum energy product of the hard-soft composites requires at least a partial inter-phase exchange coupling. The combination of a complete magnetostatic coupling and a partial exchange coupling may facilitate the development of anisotropic composite magnets with superior performance. The experimental studies found that (1) magneto-statically coupled soft magnetic phase increases the temperature dependence of the hard magnetic properties; (2) re-distribution of elements during thermomechanical treatment is a significant factor affecting the properties of anisotropic composite magnets; (3) though the refinement of the precursor powders enables certain control over the morphology and thickness of the soft inclusions, the expected advantages are overcome by the increased oxidation of the R-rich phase and/or increased inter-phase diffusion.

15. SUBJECT TERMS

16. SECURITY CLASSIFICATION OF:			17. LIMITATION OF ABSTRACT	18. NUMBER OF PAGES	19a. NAME OF RESPONSIBLE PERSON
a. REPORT	b. ABSTRACT	c. THIS PAGE			19b. TELEPHONE NUMBER (include area code)

Scientific Background: According to the conventional belief, composite magnets based on rare earth compounds blended with soft magnetic phases should necessarily have a structure refined to the nanoscale level in order to ensure improved magnetic properties. This requirement is set by the short range of magnetic exchange interactions, which are meant to be responsible for the magnetic coupling between the hard and soft magnetic phases. However, recent experiments [1,2] on composite magnets prepared by hot-pressing and hot-deformation of blends of crushed nanocrystalline $R_2Fe_{14}B$ melt-spun ribbons (where R is rare earth) and micron-size iron powders, suggested that the magnetic coupling between the hard and soft phases can also be in much coarser structures. The magnetic coupling in these composite systems is a long-range magnetostatic coupling ensured by a specific layered morphology formed during the hot-deformation process.

Objective of the Project: The aim of the work was *to fabricate and study new high-performance composite permanent magnets based on rare-earth compounds blended with soft magnetic phases.* Understanding the role of the magnetostatic interactions is important in achieving the magnetic coupling and enhanced magnetic properties in composite permanent magnets. Our research efforts were focused on:

(1) The theoretical study of magnetostatic coupling in hard / soft composites by numerical simulation.

(2) The adjustment of the composition of the R-Fe-B component in order to compensate the partial re-distribution of Fe that takes place during die-upsetting.

(3) The adjustment of the morphology of the soft inclusions through different blending techniques and use of different types of precursor powders.

Results

1. Numerical Simulation of Magetostatic Coupling

In the model [1], a magnet was represented by a 3D array of uniformly magnetized cube-shaped elements. Both the magnetization and magnetic field were assumed to be parallel to the common easy magnetization direction z. Two types of magnetic elements were considered: the soft magnetic element had a reversible magnetization curve and no coercivity, while the hard magnetic element representing the phase with a high intrinsic coercivity H_c^{hard} had a rectangular demagnetization curve. The magnetizations of all the elements in the array (ensemble) were calculated assuming the effective field at the ith element H_i to be given by,

$$H_i = H + \sum_{j \neq i} F_{ij} M_j , \qquad (1)$$

where the second term is the sum of stray fields generated by the other elements. The coefficients F_{ij} describe the z-components of the effective interaction fields in the array of contiguous uniformly magnetized cubes. After finding by iterations the equilibrium magnetization state of the ensemble, a correction has been made for the ensemble self-demagnetizing field (the demagnetization factor of 1/3).

2

Calculated demagnetization curves of the ensembles composed of hard and soft elements showed that the arrangement of the soft elements into layers parallel to z does not lead to a magnetic coupling with the hard phase. For randomly distributed elements, a significant coupling between the phases appears. When the soft elements form layers perpendicular to z, the hard and soft phases appear to be fully magnetically coupled. Demagnetization curves calculated for different volume fractions of the hard and soft layers with the soft layers perpendicular to the direction of magnetization showed that even though the saturation magnetization of the ensemble increases with increasing the volume fraction of the soft phase, the remanence value remains close to that of the hard phase. The curve rectangularity, maximum energy product and coercivity decrease with adding the soft phase. Thus, the theoretical simulation explains the magnetic coupling observed in the hot-pressed and hot-deformed magnets. It cannot, however, explain the observed increase in $4\pi M_r$ and $(BH)_{max}$.

In a modified model, intended to estimate the additional effect of a *partial* exchange coupling, we assumed that the outer magnetization elements of a soft inclusion are coupled with the matrix in the following way. When the "coupled" soft element i is sandwiched between the soft element j and the hard element k, its magnetization M_i is "transitional" between M_j and M_k and is given by,

$$M_i = \frac{M_s^{soft}}{2}\left(\frac{M_j}{|M_j|} + \frac{M_k}{|M_k|}\right) \tag{2}$$

When an incomplete exchange coupling was enabled during the simulation, the assembles with soft layers perpendicular to z exhibited not only the unitary demagnetization behavior, but also the monotonic enhancement of the remanence with increasing the fraction of soft phase. It should be noted that because we did not solve the micromagnetic problem, the theoretical results related the partial exchange coupling should be considered as rough estimates.

When the thickness of exchange-coupled soft inclusions exceeds the critical width of a few nanometers, a small demagnetizing field leads to magnetization reversal in the middle part of the inclusion [2]. Even if this magnetization reversal is reversible (the so-called "exchange spring" behavior) it strongly worsens the performance of the magnet. This makes the hard-soft exchange-coupled magnets so much sensitive to the size of the soft grains and, in particular, it seriously complicates the development of anisotropic hard-soft magnets. In magnets with a layered morphology, the inter-phase magnetostatic interaction provides a complete magnetic coupling between the hard and soft phases preventing the reversal of the middle parts of the soft layers. The very strict requirements for the size of soft magnetic inclusions will be, therefore, effectively relaxed, though enhancement in the hard magnetic properties is expected to increase with decreasing the size of the inclusion (as the larger part of the inclusion is coupled with the matrix through the exchange interaction). It should be noted that the composites with complete magnetostatic coupling and partial exchange coupling between the hard and soft phases are not expected to have the high $(BH)_{max}$ for predicted the fully exchange coupled nanocomposites [3], but they can still surpass the best existing magnets. It is also obvious that because the internal demagnetizing field acting on the hard phase in the magnetostatically coupled composites is proportional to M_s of the soft phase, the hard phase must have an increased H_c.

3

2. Effect of the Hard Phase Coercivity

The above theoretical study is consistent with our earlier observation [1] that in magnetostatically coupled systems the benefits of adding the soft phase can be expected only if the hard phase has a large H_c (because it must withstand the additional stray fields generated by the soft phase). To verify this concept, we compared the maximum energy products at different temperatures for α-Fe-free and α-Fe-added die-upset magnets of the standard (not enhanced) room-temperature H_c (Fig. 1). Indeed, as the coercivity increases with cooling, the difference in $(BH)_{max}$ becomes smaller, and at 150 K the composite magnet exhibits the better performance than α-Fe-free one (the decline of properties at the lower temperatures is caused by the spin-reorientation transition at 130 K). However, because the project was not aimed at cryogenic-application magnets, in the rest of our study we had to employ the H_c-enhanced hard magnetic alloys (the enhancement was typically achieved by substituting as much as 25% Dy for Nd in the Nd-Fe-B phase).

3. Correction of Composition for Re-Distribution of Fe

At the temperatures of hot-consolidation and especially die-upsetting, certain diffusion of elements is unavoidable. It fact, diffusion in the liquid R-rich phase is believed to be a mechanism for the texture development in R-Fe-B alloys. However, because the $R_2Fe_{14}B$, R-rich and α-Fe phases cannot coexist in equilibrium R-Fe-B alloys, the diffusion also changes the microchemistry of the composite magnets.

In out earlier work [1], we measured the weight percentage of the α-Fe phase in the $Nd_{14}Fe_{79.5}Ga_{0.5}B_6$ / Fe and $(Nd_{0.75}Dy_{0.25})_{14}Fe_{79.5}Ga_{0.5}B_6$ / Fe die-upset anisotropic magnets. Fig. 2(a) presents the results of the measurements for the magnets die-upset at 900 °C. The actual concentration of the α-Fe phase is always lower than the weight fraction of the added iron powder (the deviation from the dash). Assuming that the missing Fe atoms had diffused into the R-Fe-B matrix, we calculated its average composition for the die-upset composite magnets, and the results are shown in Fig. 2(b). The average R content of the R-Fe-B constituent decreases by more than 0.5 at.%. This is equivalent to a decrease of the amount of the R-rich phase (reaction of this phase with the Fe atoms produces more $R_2Fe_{14}B$ phase), and may significantly affect the hard magnetic properties. Though in our case the R-Fe-B matrix always remains enriched with R over the $R_2Fe_{14}B$ stoichiometry (11.8 at.%), the minimum necessary excess of R can be found only from experiment (part of R also forms oxides, and that part depends on the specific manufacturing conditions).

We prepared a single-component $Nd_{13.48}Fe_{80.26}Ga_{0.48}B_{5.78}$ die-upset magnet corresponding to the average composition of the Nd-Fe-B matrix of the 91% $Nd_{14}Fe_{79.5}Ga_{0.5}B_6$ / 9% Fe composite. As one can see in Table 1, the small Fe enrichment leads a dramatic decline of both the remanence and coercivity in $Nd_{13.48}Fe_{80.26}Ga_{0.48}B_{5.78}$ when compared to the parent $Nd_{14}Fe_{79.5}Ga_{0.5}B_6$ magnet. It seems unlikely that the Nd-Fe-B matrix in the 91 / 9 composite (also presented in the Table 1) had so low hard magnetic properties. More likely, the Fe enrichment of the Nd-Fe-B matrix in the composite is very non-uniform and cannot be adequately simulated via a single-component magnet of the average composition. The results, however, suggest that the chemical changes associated with die-upsetting should be taken into account. We corrected the composition of the

Nd-Fe-B alloy in order to compensate the expected enrichment by 3 wt.% Fe. The new composition was $Nd_{14.55}Fe_{78.7}Ga_{0.5}B_{6.2}$, so that 91 wt.% $Nd_{14.55}Fe_{78.7}Ga_{0.5}B_{6.25}$ + 3 wt.% Fe = $Nd_{14}Fe_{79.5}Ga_{0.5}B_6$. Data presented in Table 1 confirm that such correction markedly increases the coercivity and maximum energy product of the composite magnet.
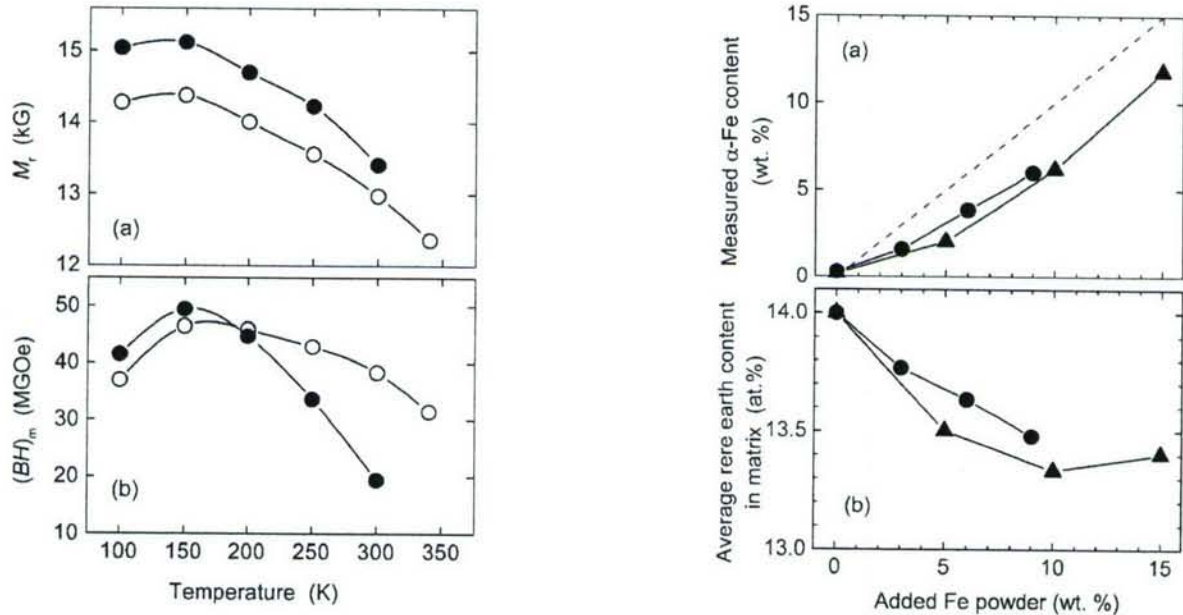

Fig. 1 (left). Temperature dependence of (a) remanent magnetization and (b) maximum energy product of die-upset magnets prepared from 100%: $Nd_{14}Fe_{79.5}Ga_{0.5}B_6$ (open circles) and blend of 94% $Nd_{14}Fe_{79.5}Ga_{0.5}B_6$ and 6% Fe (filled circles).

Fig. 2 (right). Effect of added iron powder on (a) percentage of α-Fe phase and (b) calculated R content in the R-Fe-B matrix for die upset magnets: $Nd_{14}Fe_{79.5}Ga_{0.5}B_6$ / Fe (circles) and $(Nd_{0.75}Dy_{0.25})_{14}Fe_{79.5}Ga_{0.5}B_6$ / Fe (triangles).

Table 1. Properties of die-upset magnets made from melt-spun Nd-Fe-B alloys (1 - 200 μm) with or without 9 wt.% addition of iron powder (5 - 45 μm).

Starting powders	B_r (kG)	H_c (kOe)	$(BH)_{max}$ (MGOe)
100% $Nd_{14}Fe_{79.5}Ga_{0.5}B_6$	13.8	10.6	43.6
100% $Nd_{13.48}Fe_{80.26}Ga_{0.48}B_{5.78}$	9.7	2.3	10.8
91% $Nd_{14}Fe_{79.5}Ga_{0.5}B_6$ + 9% Fe	14.0	1.8	15.6
91% $Nd_{14.55}Fe_{78.7}Ga_{0.5}B_{6.25}$ + 9% Fe	13.1	4.4	25.9

Similar results were obtained when correcting the concentration of R-Fe-B component in the 85% $(Nd_{0.75}Dy_{0.25})_{14}Fe_{79.5}Ga_{0.5}B_6$ / 15% Fe composite for re-distribution of 3.5 wt.% Fe (see Table 2). Replacing $(Nd_{0.75}Dy_{0.25})_{14}Fe_{79.5}Ga_{0.5}B_6$ by $(Nd_{0.75}Dy_{0.25})_{14.7}Fe_{78.5}Ga_{0.5}B_{6.3}$ (85% wt.% $R_{14.7}Fe_{78.5}Ga_{0.5}B_{6.3}$ + 3.5 wt.% Fe = $R_{14}Fe_{79.5}Ga_{0.5}B_6$), has doubled the coercivity of the die-upset composite and increased $(BH)_{max}$ from 24 to 27.4 MGOe. Due to the high H_c we were able to increase the amount of iron powder in the blend to 20 wt.%. The new 80%

$(Nd_{0.75}Dy_{0.25})_{14.7}Fe_{78.5}Ga_{0.5}B_{6.3}$ / 20% Fe composite is remarkable by having the *under-stoichiometric* overall composition $R_{11.3}Fe_{83.4}Ga_{0.4}B_{4.9}$, while still exhibiting the anisotriopic hard magnetic behavior. The increased α-Fe addition, however, did not increase the remanence and decreased $(BH)_{max}$.

Table 2. Properties of die-upset magnets made from melt-spun (Nd,Dy)-Fe-B alloys (1 - 200 µm) and iron powder (5 - 45 µm).

Starting powder blend	B_r (kG)	H_c (kOe)	$(BH)_{max}$ (MGOe)
85% $(Nd_{0.75}Dy_{0.25})_{14}Fe_{79.5}Ga_{0.5}B_6$ + 15% Fe	11.2	7.0	24.0
85% $(Nd_{0.75}Dy_{0.25})_{14.7}Fe_{78.5}Ga_{0.5}B_{6.3}$ + 15% Fe	11.5	13.2	27.4
80% $(Nd_{0.75}Dy_{0.25})_{14.7}Fe_{78.5}Ga_{0.5}B_{6.3}$ + 20% Fe	11.5	9.0	24.9

4. Effect of Fe-Co Additions with Different Morphologies

The Fe-Co alloys exhibit a higher saturation magnetization than Fe and, therefore, are more attractive as soft magnetic additions. The $Fe_{65}Co_{35}$ alloys were synthesized from pure Fe and Co powders by mechanical alloying (co-milling in a SPEX-8000 ball mill under argon for 200 min). The directly extracted Fe-Co powder featured irregular particles with a broad size distribution (from microns to tens of microns). This powder took approximately 86 - 88 wt.% of the initial charge. The remaining 12 - 14% could be extracted only after subsequent milling in ethanol (for approx. 20 min). Most of these particles were shaped as flakes with the very uniform thickness of about 1 µm. The blends for hot-pressed / die-upset composite magnets were prepared with both the irregular particles and flakes. The blend with irregular particles was also subjected a high-energy ball milling for 5 and 30 min in order to achieve more uniform mixing.

After hot-pressing and die-upsetting, the different Fe-Co additions used resulted in distinctly different microstructures. Die-upset magnets made with the irregular Fe-Co particles contained platelet-shaped Fe-Co inclusions typically more than 5 µm thick. In the case of Fe-Co flakes, only few inclusions were thicker than 2 - 3 µm; however, a large amount of a separated R-rich, most likely oxide, phase were present. The inclusions in the magnets made from the co-milled blends were even thinner, typically thinner than 1 µm. The magnetic properties of the composite magnets made with Fe-Co alloys are summarized in Table 3. Despite the more refined microstructure, the composite magnets made with the Fe-Co flakes do not exhibit higher remanence and their coercivity is almost two times lower than that for irregular Fe-Co particles. The co-milling of components prior to consolidation leads to an inferior texture.

Table 3. Properties of die-upset magnets made from 90 wt.% $(Nd_{0.75}Dy_{0.25})_{14}Fe_{79.5}Ga_{0.5}B_6$ melt-spun alloy and 10 wt.% $Fe_{65}Co_{35}$ mechanically alloyed addition.

Soft $Fe_{65}Co_{35}$ addition	Blending technique	B_r (kG)	H_c (kOe)	$(BH)_{max}$ (MGOe)
Powder	Shacking	11.4	9.1	26.1
Flakes	Shacking	11.4	5.1	24.3
Powder	Co-milling for 5 min (SPEX mill, argon)	8.1	6.5	10.6
Powder	Co-milling for 30 min (SPEX mill, argon)	6.7	7.6	6.6

To understand the observed effects of different Fe-Co precursors we have analyzed the spatial distribution of the elements near the soft magnetic inclusions in the die-upset magnets. The thicker Fe-Co inclusions typical of the composite magnets made with irregular Fe-Co particles have well-defined chemical boundaries for all the elements analyzed. In contrast, the thinner Fe-Co inclusions typical of the magnets made with Fe-Co flakes exhibit a distribution of Co going beyond the boundaries of the inclusions as defined via the Fe and Dy distributions. The diffusion of Co into the R-Fe-B matrix is even more pronounced in the case of the magnets made from co-milled R-Fe-B and Fe-Co components. Because cobalt deteriorates the magnetocrystalline anisotropy of the $Nd_2Fe_{14}B$ compound, such diffusion may decrease the coercivity of the magnets made with the Fe-Co flakes.

5. Effect of Fe Additions

5.1. Effect of Particle Size of Precursor Powders

Table 4 presents the properties of die-upset magnets fabricated from blends of different fractions of ground R-Fe-B alloys and different commercially available iron powders. Decrease of particle size of any of the precursors leads to a drastic decline of the magnet coercivity. When both precursor powders are of the finest grade, the remanence declines as well. The latter result may indicate the over-critical loss of the R-rich phase in the R-Fe-B powders (the certain amount of this phase is required for the successful texture development.) On one hand, the increased surface area of the finer R-Fe-B powders facilitates oxidation of the R-rich phase. On the other hand, the finer Fe particles are expected to bring a greater amount of adsorbed oxygen. In an attempt to preserve the R-rich phase, we synthesized the modified hard phase, $(Nd_{0.75}Dy_{0.25})_{14.7}Fe_{74}Co_4Cu_{0.5}Ga_{0.5}B_{6.3}$: *small* additions of Co and Cu are known to improve the corrosion resistance of the R-rich phase in R-Fe-B sintered magnets [6]. However, as the data presented in Table 5 show, this modification, though it improves coercivity of the magnets fabricated from the finest precursor powders, it further degrades the remanent magnetization.

Table 4. Properties of die-upset magnets made from differently comminuted 85 wt.% $(Nd_{0.75}Dy_{0.25})_{14.7}Fe_{78.5}Ga_{0.5}B_{6.3}$ melt-spun alloy and 15 wt.% Fe powder.

Precursor powders particle size (μm)		B_r (kG)	H_c (kOe)	$(BH)_{max}$ (MGOe)
R-Fe-B powder	Fe powder			
1 - 200	5 - 45	11.4	13.2	27.4
1 - 200	1 - 3	11.5	3.7	20.7
1 - 45	5 - 45	11.6	6.6	25.9
1 - 45	1 - 3	10.6	2.3	14.2

Table 5. Properties of die-upset magnets made from differently comminuted 85 wt.% $(Nd_{0.75}Dy_{0.25})_{14.7}Fe_{74}Co_4Cu_{0.5}Ga_{0.5}B_{6.3}$ melt-spun alloy and 15 wt.% Fe powder.

Precursor powders particle size (μm)		B_r (kG)	H_c (kOe)	$(BH)_{max}$ (MGOe)
R-Fe-B powder	Fe powder			
1 - 200	5 - 45	10.2	8.3	19.9
1 - 200	1 - 3	10.3	4.7	15.4
1 - 45	1 - 3	9.6	3.6	11.6

It is possible that the major reason for the detrimental effect of finer precursor powders is an increased diffusion through the increased interface areas.

In the next series of experiments the melt-spun R-Fe-B alloy has been ball-milled under toluene with a low-energy rotary mill and then blended with 15 wt.% iron powders of different size. Addition of 1 - 10 μm Fe particles (Table 6) led to a very significant increase of Mr and (BH)max (24% and 30% increase, respectively). It should be noted, however, that the α-Fe-free magnet had poor properties, and, when compared to our earlier results [1], the pre-milling of the R-Fe-B powder does not seem to bring an improvement. As for the "100 nm" iron powder (nominal size; the SEM characterization of the powder revealed two fraction: one of approximately 100 nm, but the other of 1 - 3 μm), it made all the properties of the composite magnet except M_r to decline. Interestingly, the SEM investigation showed that the latter magnet featured continuous layers of the α-Fe phase, typically 200 - 500 nm thick, while the α-Fe inclusions in the magnet made with 1 - 10 μm Fe particles (and showing the better properties) were thicker and shorter. Again, the compositional changes (oxidation or Fe diffusion) appear to play a more significant role than the morphology.

Table 6. Properties of die-upset magnets made from ball-milled $(Nd_{0.75}Dy_{0.25})_{14.7}Fe_{74}Co_4Cu_{0.5}Ga_{0.5}B_{6.3}$ melt-spun alloy (1 h in a rotary mill under toluene) and Fe powder.

Iron powder addition	B_r (kG)	H_c (kOe)	$(BH)_{max}$ (MGOe)
None	8.8	15.8	17.8
15 wt.% iron powder 1 - 10 μm	10.9	6.9	23.2
15 wt.% iron powder 100 nm	9.2	4.4	10.4

5.2. Effect of Blending Technique

Several attempts have also been made to achieve a more uniform distribution of the soft phase. Two of them, magnetizing the R-Fe-B powder prior to blending and *low-energy* co-milling of R-Fe-B and Fe (earlier we described the *high-energy* co-milling of R-Fe-B and Fe-Co) are summarized in Table 7.

Table 7. Properties of die-upset magnets made from differently blended 85 wt.% $(Nd_{0.75}Dy_{0.25})_{14.7}Fe_{78.5}Ga_{0.5}B_{6.3}$ melt-spun alloy (1 - 200 μm) and 15 wt.% Fe powder (1 - 3 μm).

Blending technique	B_r (kG)	H_c (kOe)	$(BH)_{max}$ (MGOe)
Shacking (as-ground powders)	11.5	3.7	21.0
Shacking (pre-magnetized R-Fe-B powder)	11.5	4.8	21.0
Co-milling for 3 h (rotary mill, toluene)	7.4	4.3	3.6

Project Summary

- The computer simulation studies based on dipolar coupling confirm a magnetic coupling between magnetically hard R-Fe-B layers and thick magnetically soft Fe layers in hot-deformed composite magnets, but do not predict any enhancement in M_r and $(BH)_{max}$.

- According to the simulation results, the enhancement in M_r and $(BH)_{max}$ in the hard-soft composites requires at least a partial inter-phase exchange coupling. The combination of a complete magnetostatic coupling and a partial exchange coupling between the hard and soft phases may facilitate the development of anisotropic composite magnets with superior performance.

- Magnetostatically coupled soft magnetic inclusions increase the temperature dependence of the hard magnetic properties.

- Re-distribution of elements, particularly Fe and Co, during thermomechanical treatment is a significant factor affecting the properties of anisotropic composite magnets. Compositions of the starting materials have to be corrected for the re-distribution in order to assure the maximum performance.

- Though the refinement of the precursor powders enables certain control over the morphology and thickness of the soft inclusions, the expected advantages are overcome by the increased oxidation of the R-rich phase and/or increased inter-phase diffusion.

- Flakes of Fe-Co alloys with a uniform thickness of approximately 1 μm can be fabricated by mechanical alloying in argon with subsequent milling in ethanol.

References

[1] A.M. Gabay, M. Marinescu and G.C. Hadjipanayis, "Enhanced M_r and $(BH)_{max}$ in anisotropic $R_2Fe_{14}B$ / α-Fe composite magnets via intergranular magnetostatic coupling," J. Appl. Phys. 99, 08B506 (2006).

[2] D. Lee, S. Bauser, A. Higgins, C. Chen, S. Liu, M.Q. Huang, Y.G. Peng and D.E. Laughlin, "Bulk anisotropic composite rare earth magnets," J. Appl. Phys. 99, 08B516 (2006).

[3] A.M. Gabay and G.C. Hadjipanayis, "Numerical simulation of a magnetostatically coupled composite magnet," J. Appl. Phys. 101, 09K507 (2007)

[4] E.F. Kneller and R. Hawig, "The exchange-spring magnet: a new material principle for permanent magnets," IEEE Trans. Magn. 27, 3588 (1991).

[5] R. Skomski and J.M.D. Coey, "Giant energy product in nanostructured two-phase magnets," Phys. Rev. B 48, 15812 (1993).

[6] M. Katter, L. Zapf, R. Blank, W. Fernengel and W. Rodewald, "Corrosion mechanism of RE-Fe-Co-Cu-Ga-Al-B magnets," IEEE Trans. Magn. 37, 2474 (2001).